Focussed on Multiaxial Fatigue and Fracture

Fatigue life assessment of a non-load carrying fillet joint considering the effects of a cyclic plasticity and weld bead shape

S. Tsutsumi, K. Morita, R. Fincato, H. Momii
Joining and Welding Research Institute, Osaka University, Japan
tsutsumi@jwri.osaka-u.ac.jp, http://orcid.org/0000-0001-2345-6789
morita@jwri.osaka-u.ac.jp, http://orcid.org/0000-0002-2345-6790
fincato@jwri.osaka-u.ac.jp, http://orcid.org/0000-0002-2345-6791
hideto.momii@estech.co.jp http://orcid.org/0000-0003-2345-6792

ABSTRACT. Fatigue life depends strongly on irreversible contributions that accumulate during cyclic loading and unloading of structures. However, the correct identification of the loading path in terms of uniaxial or multi-axial stress states, proportional or non-proportional loading is essential because these factors can significantly alter the material response. In this study, finite element analysis was conducted to assess the fatigue crack initiation life of a non-load carrying fillet joint by considering weld bead shape and a cyclic plasticity accumulation during fatigue loading, which is a main cause of crack initiation. Cyclic plasticity behaviour including cyclic hardening and softening together was investigated with an unconventional plasticity model called the subloading surface model and extended to include both elastic boundary and cyclic damage concepts. The cyclic plasticity model can capture realistic plastic strain accumulation during high cycle fatigue under macroscopically elastic stressing conditions.

KEYWORDS. Unconventional plasticity; Fatigue; Loading path; Crack initiation.

Citation: Tsutsumi, S., Morita, K., Fincato, R., Momii, H., Fatigue life assessment of a non-load carrying fillet joint considering the effects of a cyclic plasticity and weld bead shape, Frattura ed Integrità Strutturale, 38 (2016) 244-250.

Received: 30.06.2016
Accepted: 27.07.2016
Published: 01.10.2016

INTRODUCTION

As many welded structures such as bridges reach the age at which they are projected to require maintenance, techniques to calculate their fatigue life accurately and to prolong it, are needed [1]. In addition, it is also necessary to estimate the fatigue life of pre-existing structures because most structures are already damaged. Fatigue life is determined by irreversible deformations, which tend to accumulate during the life of components as a result of loading and unloading. The correct identification of the loading path is vital because different factors can alter the material response substantially [2-3].
Numerical modeling based on the finite element (FE) method has been used to predict weld-induced residual stresses [4]. Numerical techniques are an important part of most structural research because they can be used to analyze the behavior

of structures, provided that care is taken to ensure that the model is appropriate for the analysis. The elasto-plastic model used in this paper [4-6], which reproduces cyclic elasto-plastic behaviour under high or low cyclic fatigue, has already been widely used to investigate the fatigue crack initiation life of structural components.
In this study, we investigated the fatigue behaviour of a non-load carrying fillet joint under uniaxial conditions for different loading paths, while the stress path deviate from proportional one due to the geometrical complexity of the weld bead. Also, we analyzed the effects of different loading combinations on the component service life. The results were in good agreement with experimental results, although a method of predicting fatigue life under multi-axial and more generic loads has not been developed. The authors [7] suggested that it may be possible to predict fatigue life under multi-axial and variable loading conditions by using a damage parameter (H_d), which takes into account the plastic work. We examine the relationship between H_d and fatigue life by coupling the subloading surface equations with an internal damage variable. The numerical analyses were performed with two different approaches: a series of tests investigated the material response and FE analysis was applied to a steel component of a material and a non-load carrying fillet joint. The material response tests gave us information about the correlation between H_d and the fatigue crack initiation life, which was used in the non-load carrying fillet joint simulations to reproduce the experimental results provided by the Japanese Society of Steel Construction (JSSC).

CONSTITUTIVE EQUATIONS AND NUMERICAL PROCEDURE

Constitutive equations of the material

The extended subloading surface model [4-6] describes the generation of plastic strain within the yield surface (subloading surface), which can be obtained through a similarity transformation from the conventional yield surface (referred to as the normal-yield surface in Fig. 1). Classical theories distinguish elastic and plastic regions, allowing an irreversible stretch only in the plastic region. In contrast, the subloading surface model abolishes the separation into domains, stating that a plastic response can be realized for every change in the stress state that satisfies the loading criterion. Furthermore, the use of a mobile similarity center, which is a function of the plastic strain, makes this theory particularly suitable for studying cyclic mobility problems. A detailed explanation of the model features is beyond the scope of this paper, and the reader is referred to Refs. [4-6] for a more complete discussion.
The damage variable, modelled as a phenomenological loss of stiffness, was coupled with the elasto-plastic equations according to the theory proposed by authors [7]. The constitutive equations of the extended subloading surface model were modified to include the progressive relaxation of the material induced by the damage, D, which becomes function of a special variable of the cumulative plastic strain, H_d, of

$$D(H_d) = (1 - d_2)\left[1 + \left(\frac{d_1}{H_d}\right)^{d_3}\right]^{-1} \tag{1}$$

where d_1, d_2, and d_3 are material parameters that regulate the damage rate evolution, as shown in Fig. 2, and must be calibrated depending on the material.
An example of a feature of the new theory is shown in Fig. 3, in which progressive material relaxation induces the opening of the loops during fully reversible cyclic loading. Fig. 3 shows the experimental stress-strain evolution, whereas Fig. 4 shows the numerical evolution calculated with the same boundary conditions and with the material parameters in Tab. 1.

Material parameters	Value	Material parameters	Value
E	206,000 [MPa]	Re_0	0.4
ν	0.3	$a1$; $a2$; $a3$	2.5; 740; 3
u	10,000	$k1$; $k2$; $k3$	0.316; 0.5; 8
F_0	350 [MPa]	d_1; d_2; d_3	0.0063; 0.0045; 1.6

Table 1: Material parameters used in this paper

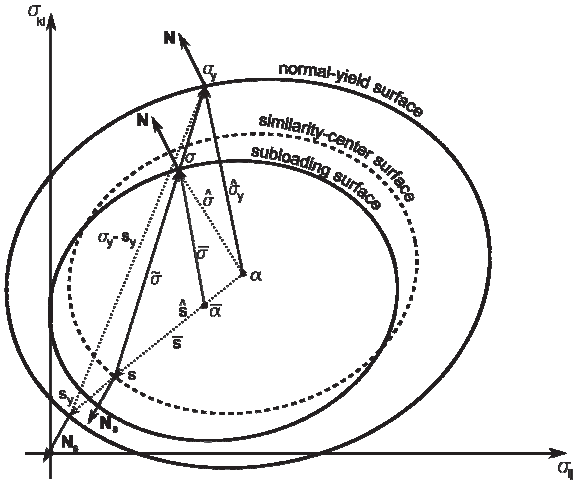

Figure 1: Sketch of the subloading and normal yield surfaces in the stress space.

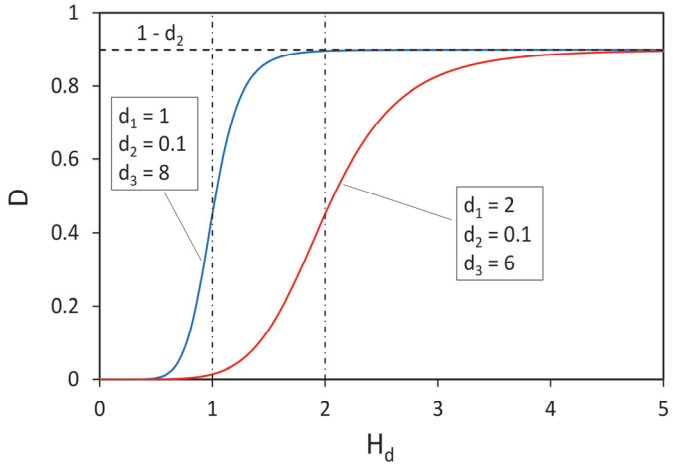

Figure 2: Damage evolution for two sets of material parameters.

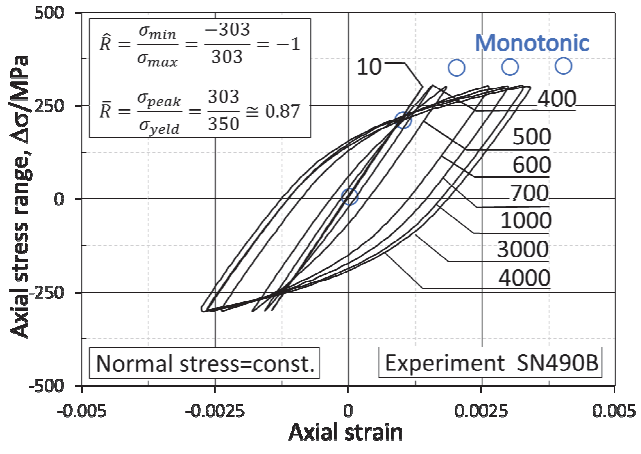

Figure 3: Experimental stress-strain curves (R = -1, σ_{max} = 303/monotonic).

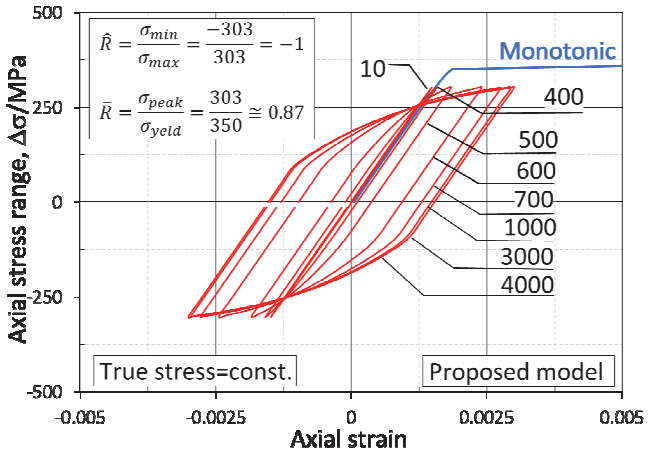

Figure 4: Numerical stress-strain curves (R = -1, σ_{max} = 303/monotonic).

Constitutive equations of the material

Preliminary single-quadrature point numerical code was created implementing the constitutive equations of the subloading surface model coupled with the damage variable to verify the material response. Numerical simulations were performed considering cyclic loading with a constant stress range and loading ratios (R = -1/0/0.5), and two analyses were performed where the loading amplitude varied during cycles.

The algorithm was used in commercial FE code (Abaqus/Standard ver. 6.14-4) via a subroutine for studying real steel component behavior. Fig. 5 shows the geometry and mesh adopted in the FE simulations of a non-load carrying fillet joint test, where the welded toe shape is assumed as rounded. For simplicity, 1/4 of the whole bar was modelled owing to the double symmetry of the sample. A mesh refinement (0.05 mm minimum element dimension) was performed around the welding toe, where the largest stress concentration tends to appear. A total of 4262 plate elements (plane strain assumption) were used in the discretization, amounting to a total of 4356 nodes. The numerical simulations were conducted for cyclic loading with a constant amplitude (R = 0, σ_{max} = 180 MPa), and four combinations of variable loading amplitudes.

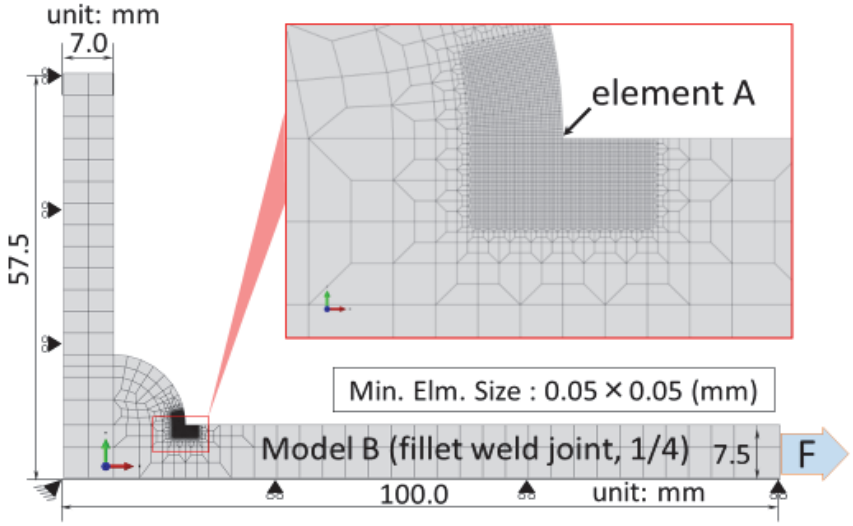

Figure 5: Model and boundary conditions used.

Material	σ_{max} changes every 100 cycles (R = -1)			
	Name	Order of loading [MPa]	H_d = 1 [cycles]	
	mat.UpDown	303 →340→303→268→303	1054	
	mat.DownUp	303 →268→303→340→303	1178	
Weld joint	σ_{max} changes every 25 cycles (R = 0)			
	Name	Order of loading [MPa]	D = 1 [cycles]	H_d = 1 [cycles]
	W.UpDown1	180→300→180→100	15,095	408
	W.UpDown2	300→180→100→180	14,567	389
	W.DownUp1	180→100→180→300	15,568	422
	W.DownUp2	100→180→300→180	15,124	409

Table 2: Variable loading conditions and crack initiation life

RESULTS AND DISCUSSION

Material simulation with single-quadrature point code

We obtained preliminary results with single-quadrature point code where the input data for stress and strain are introduced directly to give perfect uniaxial loading conditions. Fig. 6 shows the S-N curves obtained for the three constant ratio tests by reporting the number of cycles necessary for the H_d variable to reach a value equal to 1 or 10 under different stress ranges.

The R = -1 case (fully reversible load) showed good agreement with previous experimental data for SM490B steel [8] when H_d = 1 was assumed as a criterion for evaluating the fatigue life, whereas the number of cycles was overestimated slightly when H_d = 10. Therefore, two additional tests were conducted with H_d = 1 for R = 0 and 0.5. Both of the curves showed that fewer cycles were required to fulfil the condition H_d = 1, although the number of cycles was lower for R = 0.5.

Further simulations were performed with fully reversible loading (R = -1), but varying the stress amplitude every 100 cycles. Figs. 7 and 8 show S-N curves obtained for two loading paths, mat.UpDown and mat.DownUp. Both of the tests stopped when H_d reached unity. The first path had a shorter fatigue life compared with the constant stress analysis (black line in Fig. 6.), whereas the second path had a longer fatigue life.

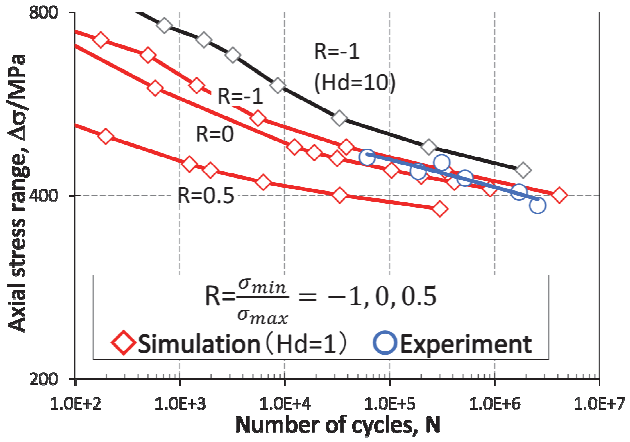

Figure 6: S-N curves at H_d = 1.

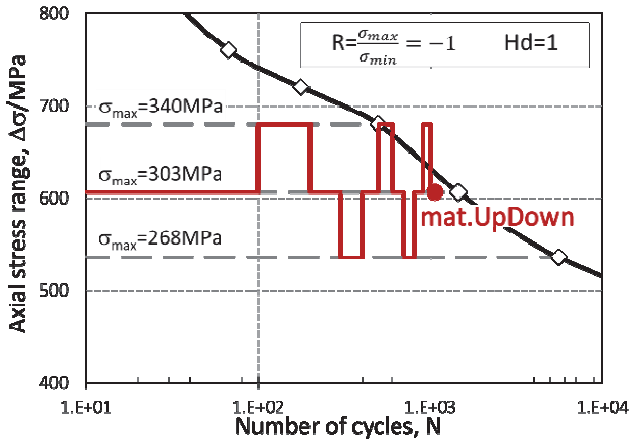

Figure 7: S-N curves in mat.UpDown (σ_{max} = 303→340→303→268→303).

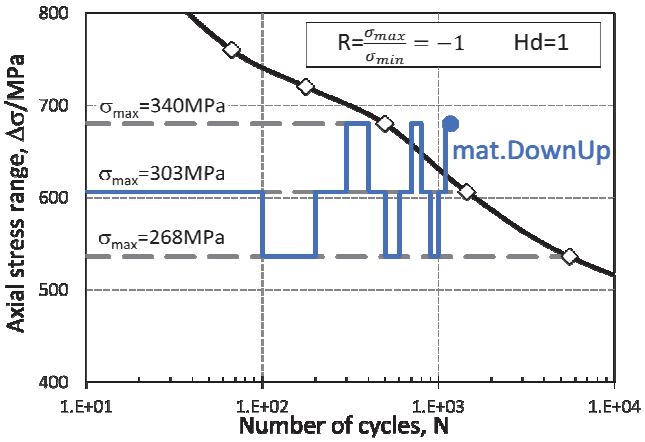

Figure 8: S-N curves in mat.DownUp (σ_{max} = 303→268→303→340→303).

FE simulation of fatigue test on the non-load carrying fillet joint

Next, the model was used in FE simulations to study the fatigue life of a non-load carrying fillet joint. Only the R = 0 case was considered to compare the results against experimental data provided by the JSSC. Loading procedures of a constant stress range and combinations of varying amplitude loads during cycles were investigated (Tab. 2). Only the paths W.UpDown1 and W.DownUp1 are discussed here. Fig. 9 shows the stress-strain curves obtained for element A in an enlargement of Fig. 5. The plastic contribution generated in the W.UpDown1 case was bigger than that induced with a constant stress range or in the W.DownUp1 path. This result is particularly relevant for the expected fatigue life of the components, as shown in Fig. 10 and the last two columns of Tab. 2. Fatigue life was estimated by using Eq. 2 based on the cumulative damage rule (D in Fig. 10) and an equation based on the total strain (H_d in Fig. 10).

$$D = \sum \frac{n}{N_{const.}}, \quad N_f = \frac{\sum n}{D} \tag{2}$$

Here, n is the number of cycles in each range of amplitude, N_{const} is the crack initiation life under constant loading estimated from the strain ranges [9], and N_f is the fatigue life proposed in this paper.

In both scenarios, the W.UpDown1 path has a shorter fatigue life than the W.DownUp1 path, whereas the estimated fatigue life is longer for a constant loading. Comparing the two fatigue life estimation methods shows that the method that uses H_d produces shorter fatigue lives than the method using the cumulative damage criteria.

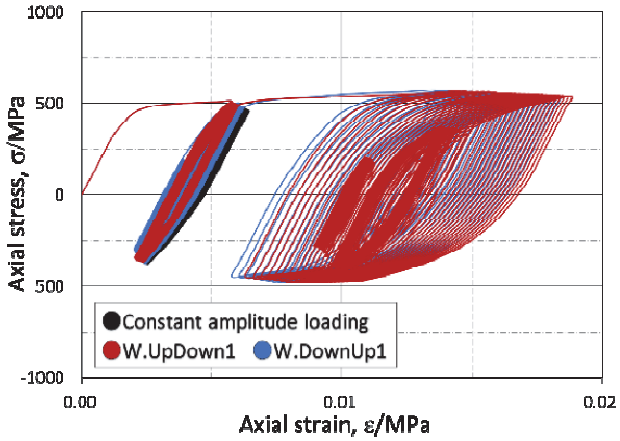

Figure 9: Stress-strain curves at element A (constant amplitude loading/variable loading).

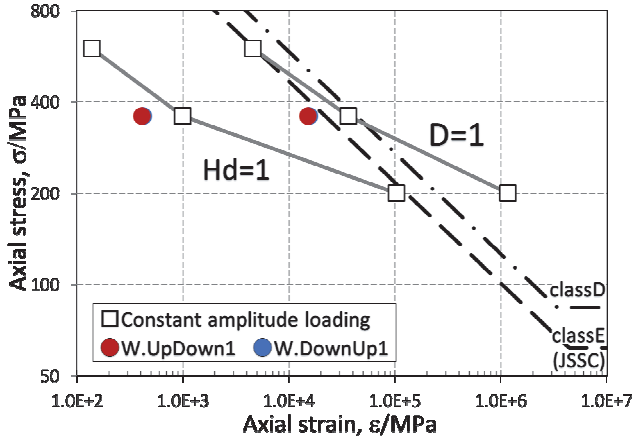

Figure 10: S-N curves at element A (constant amplitude loading/variable loading).

CONCLUSIONS

We investigated the fatigue life of metal structures with an unconventional plasticity model combined with a damage variable that includes the plastic work. We drew the following conclusions from the results.

Material simulation tests

(a) The R = -1 under constant loading case agreed well with previous experimental data [5] when H_d = 1 is assumed as the fatigue life criterion.

(b) The number of cycles necessary for fulfilling the condition H_d = 1 was sensitive to the stress ratio used, and the number of cycles decreased as the ratio increased from R = -1 to 0 and 0.5.

(c) Varying the load amplitude of a loading path for a number of cycles is also a key factor in the fatigue life. The mat.UpDown case had a shorter fatigue life compared with the constant stress analysis, whereas the loading path mat.DownUp had a longer fatigue life.

(d) The plastic contribution generated in the W.UpDown1 case was bigger that the contribution induced with a constant stress range or in the W.DownUp1 case.

(e) The fatigue life based on H_d was shorter than the fatigue life based on the cumulative damage rule.

REFERENCES

[1] Byers, W.G., Marley, M.J., Mohammadi, J., Nielsen, R.J., Sarkani, S., Fatigue reliability reassessment procedures: state-of-the-art-paper, J. Struct. Eng., 123(3) (1997) 271-276. doi:10.1061/(ASCE)0733-9445.

[2] Kainuma, S., Mori, T., A fatigue strength evaluation method for load-carrying fillet welded cruciform joints, Int. J Fatigue, 30 (2006) 864-872. doi:10.1016/j.ijfatigue.2005.10.004.

[3] Kainuma, S., Mori, T., Study on fatigue crack initiation point of load-carrying welded cruciform joints, Int. J Fatigue, 30 (2008) 1669-177. doi:10.1016/j.ijfatigue.2007.11.003.

[4] Hashiguchi, K., Tsutsumi, S., Elastoplastic constitutive equation with tangential stress rate effect, Int. J Plasticity, 17 (2001),117-145. doi:10.1016/S0749-6419(00)00021-8.

[5] Hashiguchi, K., Elastoplasticity theory. Lecture notes in applied and computational mechanics, F. Pfeiffer, P. Wriggers (Eds.), Springer, Berlin, Germany, 42 (2009).

[6] Hashiguchi, K., Subloading surface model in unconventional plasticity, Int. J. Solids Structures, 25 (1989) 917-945. doi:10.1016/0020-7683(89)90038-3.

[7] Tsutsumi, S., Murakami, K., Goto, K., Toyosada, M., Cyclic Stress-Strain Relationship during High Cycle Fatigue Process: Elastoplastic Constitutive Model Introducing Cyclic Damage Effect, Journal of the Japan Society of Naval Architects and Osean Engineers, 7 (2008) 243-250.

[8] Miki, C. Fatigue and Fracture of Bridges, Asakura Publishing, Japan (2011) 144.

[9] The Society of Materials Science. The Handbook of Fatigue Design, Japan, (1995) 123-125.